

Fault Section Identification for Line having TCSC at Mid-point

Ashok Manori

Department of EEE NIT Delhi
Narela New Delhi

Manoj Tripathy

Department of EE IIT Roorkee
Roorkee

Hari Om Gupta

JPIIT Noida,
Noida

Abstract—This paper presents a fault section identification algorithm for the protection of transmission line having TCSC in the middle of line. Wavelet Transform (WT) explores the different frequency signals present in fault current, which are analyzed by an optimal Radial Basis Function Neural Network (RBFNN) to identify the faulty section of transmission line. Simulation results clearly indicate the advantage of the application of HPF for identification of fault sections. Compensated transmission networks having Thyristor Controlled Series Compensator (TCSC), in the middle of line, have been considered in PSCAD/EMTDC software to create faults and a WT-RBFNN program in MATLAB classifies the fault section.

Keywords- Flexible alternating current transmission system, radial basis function, transmission line, and wavelet transform.

1. INTRODUCTION

FACTS controllers are connected throughout the complete length of transmission line but the preferred location is at the middle of the line because voltage sag is maximum at that point [1][2]. However, the protection of transmission line becomes a challenging task for protection engineers if FACTS controller is placed at the middle of transmission line [3], [4].

Impact of series and shunt compensators on protection of transmission line with respect to security and reliability issues are explained in ref. [4][3], which clearly indicates that FACTS devices created severe reaching problems if a fault occurs in upstream section of line. Various fault distance estimation techniques have been suggested which calculate the series compensator voltage in terms of current flowing through it by using artificial neural network (ANN) [5]. WT based boundary protection classifies the internal and external fault in series compensated transmission line [6]. WT based techniques analyze the signals which are different for internal and external faults, but the reliability of technique is compromised for various operating conditions of compensator [7], [8]. A combined S-Transform and Logistic Model Tree based technique has been presented by Zahra Moravej et al. but the results are not discussed for varying compensation level of TCSC [9]. Support Vector Machine (SVM) classifier analyzes the harmonic content present in the current to identify internal and external fault [10]. SVM combined with WT has proved to be an effective tool in fault section identification in series compensated transmission line [11]. Performance of distance protection of shunt compensated transmission line having SVC and STATCOM is improved by adjusting the over-reaching and under-reaching permissive limit of relay [12]. An accurate fault location estimation technique in transmission line having STATCOM is presented in ref. [13], which uses synchronized measurement of voltage and current at both ends of line.

Mid-point compensated transmission line has two line sections, one *downstream section* (section-I) and another *upstream section* of line (section-II). In this work, fault section is identified in compensated line by a combined WT-Radial Basis Function Neural Network (WT-RBFNN) based technique which takes less time to analyze the pattern and select the faulty section. WT decomposes all the frequency bands present in fault current signal and RBFNN analyzes the frequency patterns for different fault sections to classify the faulty section.

2. TEST SYSTEMS

A 600 MVA, 230kV, 50 Hz, 320 km long a double fed transmission test system is used to test WT-RBFNN based section identification algorithm in compensated transmission line. Rated line current is 1.5 kA for 230kV line. Per km sequence impedances of 230 kV transmission line in ohms are: ($Z_1 = 0.0362 + j0.508$, $Z_2 = 0.0362 + j0.508$, $Z_0 = 0.365 + j1.33$) [14], [15]. TCSC is connected at the middle of transmission line at the PCC. A second order HPF is also connected at the PCC to filter high frequency above 1 kHz. Section identification algorithm is tested on line having mid-point TCSC. Mid-point compensator divides the transmission line into two sections, first one downstream to the compensator and another upstream to the compensator. Brief about the mid-point series compensated line with filter is given in following subsections:

2.1 TCSC

TCSC is connected along with a filter at the PCC as shown in Fig. 1(a). Per phase maximum TCSC capacitor rating is 110Ω with compensation varies from 0 % to 70 %. Thyristors nominal current rating is 2.5 kA and blocking voltage is 5.5kV for 230kV lines. In PSCAD 3-phase TCSC is used to generate data. A single phase TCSC installed on one phase is shown in Fig. 1(b), three similar single-phase TCSC have been used for each phase.

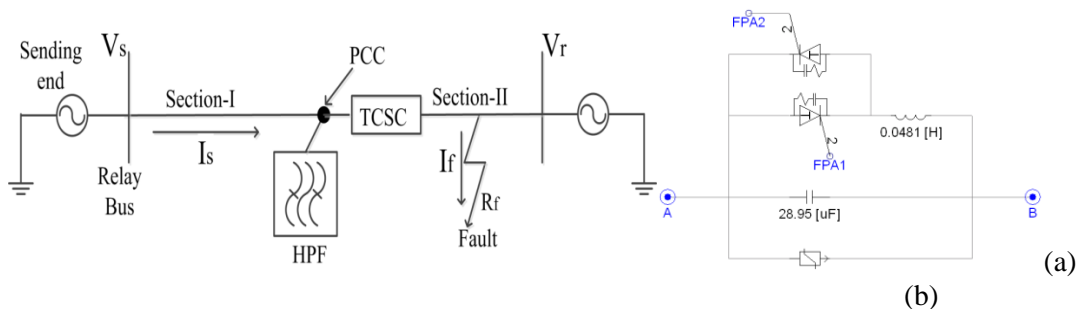


Fig.1. (a) Transmission line having TCSC (b) Per phase TCSC module in PSCAD/EMTDC

Capacitor values are calculated for different compensation levels. For particular value of series capacitance, firing angle of thyristor is kept near 85o-90o for full capacitive compensation.

2.2 High Pass Filter (HPF)

A second order HPF is also designed for the cutoff frequency of 1 kHz. Fault current contains high frequency signals from 1 to 80 kHz [16]. HPF filter out all the high frequency signals at the PCC generated due to fault in section-II. Filtered high frequency (HF) signals are shown in Fig. 2. Designed HPF is represented by eq. (1), $X(s)$ and $Y(s)$ are the input and output to the filter respectively.

$$\frac{Y(s)}{X(s)} = \frac{G \left(\frac{s}{\omega_c} \right)^2}{1 + 2\xi \left(\frac{s}{\omega_c} \right) + \left(\frac{s}{\omega_c} \right)^2} \quad (1)$$

Where, G = Gain, 1

ω_c = Characteristics frequency, 1 kHz

ξ = Damping ratio, 0.98

s = Laplace operator

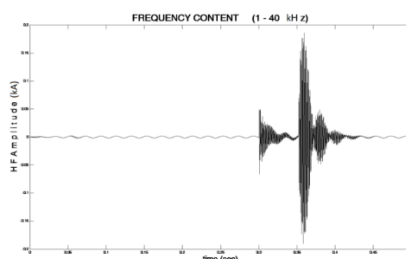


Fig. 2. High frequency content present in fault current.

3. SIGNAL PROCESSING

3.1 Wavelet Transform

WT is a powerful wave analyzing tool introduced by Jean Morlet in 1982[17]. WT provides the time localization of frequency components presents in a signal[7]. Wavelets is a family of functions constructed from translations and expansions of a function called the mother wavelet ' $\psi(t)$ ' which average value is always zero and can be given by (2):

$$\psi_{a,b}(t) = \frac{1}{\sqrt{2^a}} \psi\left(\frac{t-b*2^a}{2^a}\right) \text{ Where, } a, b \in \mathbb{R}, a \neq 0 \quad (2)$$

In Discrete Wavelet Transform (DWT) the mother wavelet is scaled by two that is provided by (3), where $x(t)$ is the signal to be analyzed. All the wavelet functions used in the transformation are derived from the mother wavelet through translation and scaling.

$$\psi_{a,b}(t) = \frac{1}{\sqrt{2^a}} \int_{-\infty}^{+\infty} x(t) \psi\left(\frac{t-b*2^a}{2^a}\right) dt \quad (3)$$

The parameter ' a ' is the scaling parameter and it measures the degree of compression. The parameter ' b ' is the translation parameter, which determines the time location of the wavelet.

In DWT, signals are discretely sampled. There are many types of mother wavelets such as Harr, Daubichies (db), Coiflet (coif), Biorthogonal (bior), Reverse Biorthogonal (rbio) and Symmlet (sym) wavelets etc. The choice of mother wavelet plays a significant role in detecting and localizing different types of fault transients. The choice also depends on a particular application. For short and fast transient disturbances, which generally occur in transmission line during fault, db4 is better and chosen for the proposed section identification algorithm[6]. The resolution of the signal, which is a measure of the amount of detail information in the signal, is determined by the filtering operations, and the scale is determined by up-sampling and down-sampling (subsampling) operations. One of the most important properties of DWT is Multi-Resolution Analysis (MRA) in which input signal resolve into thinner frequency band and each resolution is twice the previous one. Brief about the MRA technique is given in next sub-section.

3.1.1 Multi-resolution Analysis

MRA is a very useful implementation of DWT. In this analysis original sampled signal $x(n)$ is passed through a high pass filter $h(n)$ and a low pass filter $l(n)$ as shown in Fig.3[16]. Then the outputs from both filters are decimated by 2 to obtain the detail coefficients (D1) and the approximation coefficients (A1) at level one. The approximation coefficient is sent to the second stage to repeat the procedure for next level. Finally, the signal is decomposed at the expected level. In the case shown in Fig.3, if the original sampling frequency of signal is F , the signal information captured by D1 is a higher frequency band in between $F/4$ and $F/2$ at level 1. D2 captures lower frequency band information in between $F/8$ and $F/4$ at level 2. D3 captures the information between $F/16$ and $F/8$ and A3 retains the rest of the information of original signal between 0 and $F/16$. In this study detailed coefficients D1 to D4, at level one to four respectively are used for fault detection and classification algorithm.

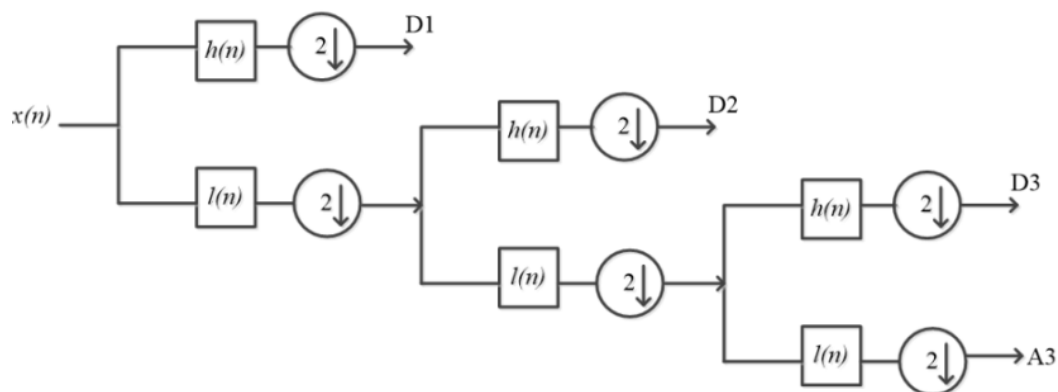


Fig3. Wavelet Multi-Resolution analysis.

3.2 Radial Basis Function Neural Network (RBFNN)

RBFNN is a feedforward neural network which is trained by supervised learning algorithm. It has become a very dominant tool to many technical problems because of its collective approximation capability and fast learning speed. It is typically configured as three layers with a single hidden layer of units whose activation function is selected from a class of functions called basis functions. The numbers of nodes in input layer are same as the dimension of input vector. All the hidden layer nodes are directly connected to input layer nodes. The hidden layer basis function has a parameter center which can be represented by a vector of size same as input vector. The inputs to the hidden layer are the linear combinations of scalar weights and input vector $x = [x_1, x_2, \dots, x_n]^T$ where 'n' is number of input. Thus the input vector 'x' becomes the input to each neuron in the hidden layer. The incoming input vectors are mapped by the radial basis function in each hidden nodes. Each hidden node represents a single RBF and computes a Gaussian kernel function of 'x'. Gaussian kernel function is considered as activation function, as suggested in [17]. The radial distance 'd_i' between the input vector 'x' and the center of the basis function 'c_i' is computed for each unit 'i' in the hidden layer as using the Euclidean distance.

$$d_i = \|x_i - c_i\| \quad (4)$$

$\phi_i(x)$ is the hidden layer output of the i^{th} hidden node which can be given as [18][19]:

$$\phi_i(x) = \exp \left[-\frac{1}{2} \sum_{j=1}^n \frac{\|x_j - c_{ij}\|^2}{\sigma_i^2} \right] \quad (5)$$

Where, c_i and σ_i denotes the center and width of the i^{th} hidden node respectively.

The output layer produces a vector $y = [y_1, y_2, \dots, y_m]$ for 'm' outputs by linear combination of the outputs of hidden nodes to produce the final output, which is given by (6).

$$y = \sum_{i=1}^k w_i \phi_i(x) \quad (6)$$

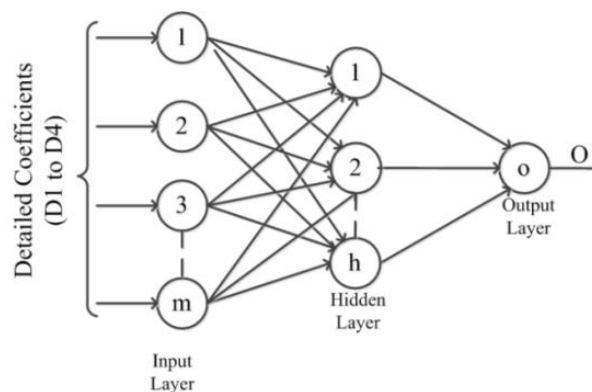


Fig.4. Typical RBFNN structure.

Where, w_i denotes the hidden-to-output weight corresponding to the i^{th} hidden node and 'k' is the number of hidden nodes. In pattern classification applications the output of the radial basis function is limited to the interval (0, 1) by the sigmoidal function (7):

$$O_m(x) = \frac{1}{1 + \exp[-y_i(x)]} \quad (7)$$

The structure of multi neurons three layered radial basis function neural network is shown in Fig. 4.

4. PROPOSED SECTION IDENTIFICATION ALGORITHM

Complete fault section identification algorithm has been shown in Fig.5. Current transformer takes three phase current signal at the sending end relay bus which is further sampled for signal processing. Wavelet based relay monitors all the three phase currents in healthy and faulty conditions individually.

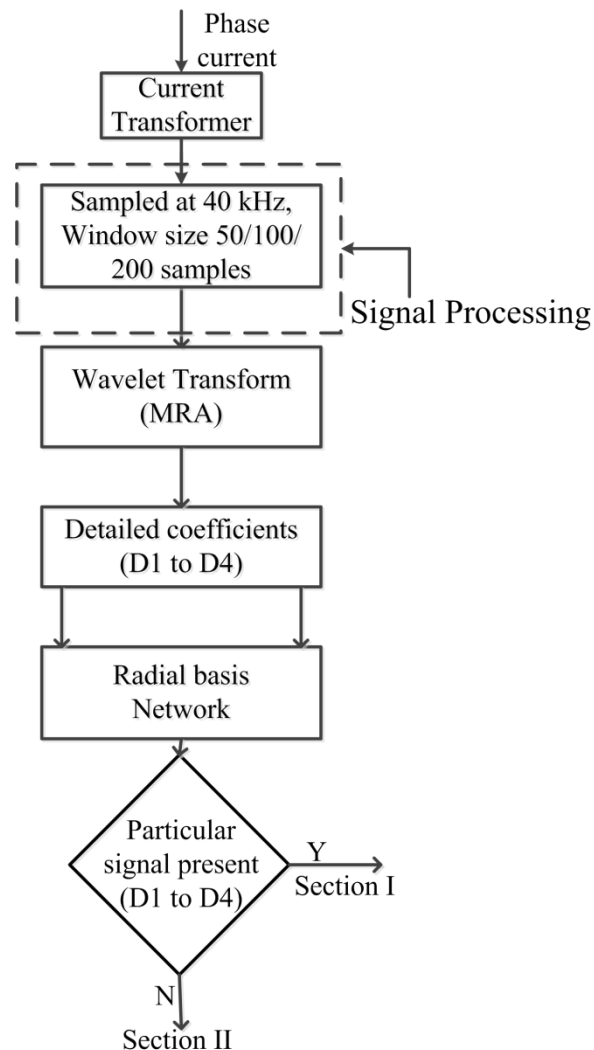


Fig.5. Proposed fault section identification algorithm.

Any transmission line fault signal has various frequency signals up-to 80 kHz [16]. Sampling frequency is selected as 40 kHz and HPF cut-off frequency is 1 kHz, therefore MRA decomposition selected up-to level four to analyze signals in between 1.25 to 40 kHz. DWT-MRA decomposes the input current into the different frequency band up to level 4 (detailed coefficients D1 to D4) by MRA techniques. Mother wavelet 'db4' is better for short and fast transient disturbances, which generally occur in transmission line during fault, and chosen for the proposed section identification algorithm. The output detailed coefficients are given as input to the designed RBFNN classifier which decides whether the particular frequency signal is present or not in the input fault current. If high frequency signals are present in the fault current the section identification algorithm decides the fault occurred in the section-I or if they are absent it decides fault occurred in section-II. Section identification is one of the most important tasks to protect mid-point compensated line. After identifying the faulty section, next step is to design an adaptive protection scheme for the fault in section-II.

5. RESULTS AND DISCUSSION

To test the reliability and security of the proposed universal fault section algorithm for mid-point compensated transmission line, several power system operating conditions are considered. WT-MRA technique extracts several fault patterns on both the sides of mid-point compensator. Mother wavelet 'db4' is chosen for the proposed section identification algorithm. Algorithm is tested for series mid-point compensated transmission line. Installation of HPF at the PCC removes the uncertainty in the filtering of high frequencies

through compensator itself which improves the reliability of the algorithm. To advise the universality of the proposed algorithm, system voltages is taken as 230kV and series compensated transmission lines are taken. Fig. 6 shows the MRA frequency patterns (D1 to D4) during faults conditions for section-I and section-II in the line having TCSC. Fig. 6(a) indicates the MRA decomposition of the current signal if fault occurred in section-I. In such case HPF does not fall in the fault loop i.e. no filtering takes place and all the high frequency signals are present in the MRA decomposition with high amplitude. While Fig. 6(b) indicates the same patterns for section-II fault in which HPF fall in the fault loop and filtering takes place. In such condition the amplitude of high frequency signals is very less or absent. In both the cases signals are compared after the instant of fault indicated in the figure. In all the taken conditions fault signal starts at $(1.2 \times 10^4)^{\text{th}}$ sample. Results taken with 50 % compensation for 230 kV system illustrated in Fig. 6.

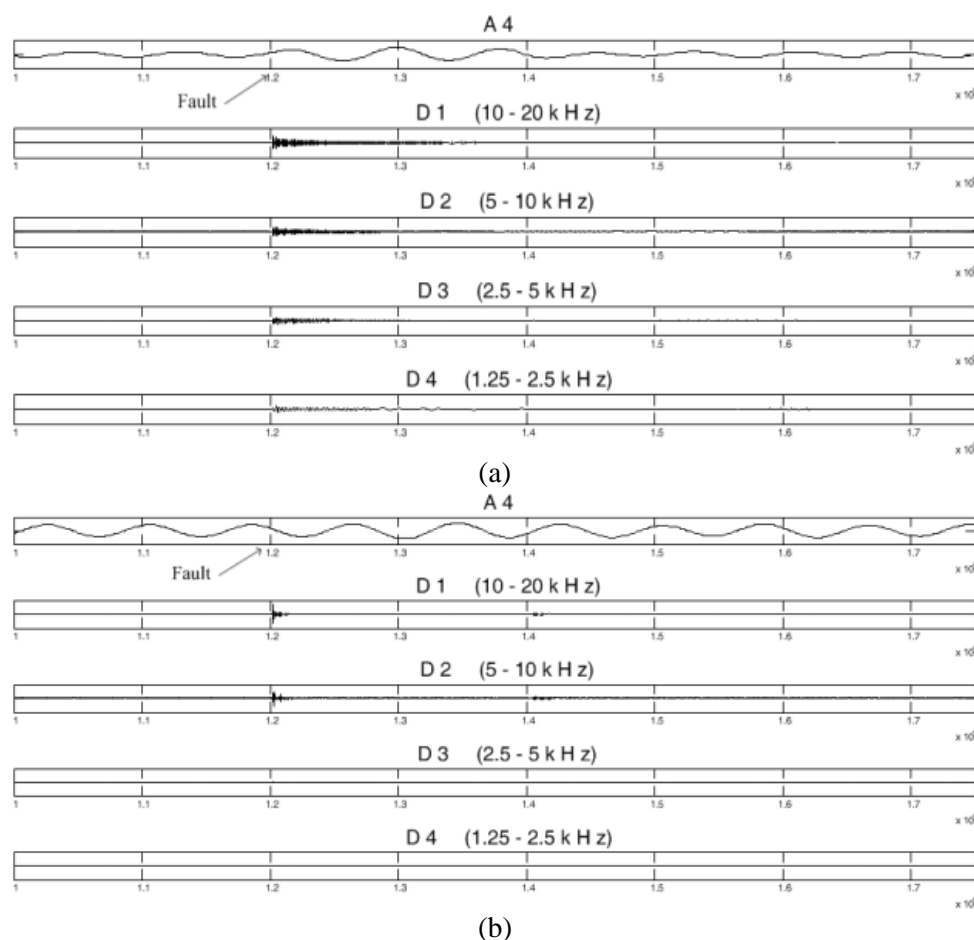


Fig. 6. MRA frequency patterns D1 to D4 for 230kV line having TCSC and faults in section (a) I (b) II.

Fig.6 compares the MRA decomposed high frequency signals generated during fault in section-I and section-II respectively. Application of HPF is indicated in Fig. 6, which filters out high frequency signals if the fault occurred in section-II. Therefore, after the fault instant the amplitude of high frequency signal is higher in section-I as compared to section-II. It is clear from result that the magnitude of the high frequency components generated due to fault in section-I is higher than section-II. Regardless the system configuration, HPF filter out the high frequency components at the PCC and high frequencies amplitude are either missing or less in section-II faults. Radial basis network is trained by detailed coefficients to decide whether the fault in section-I or section-II. Magnitude of all the detailed coefficients from D1 to D4 in section-II is clearly less than the section-I; therefore out of four patterns (D1 to D4) any pattern can be used as input for RBFNN. To

provide the required training and testing data sets, various faults are created at several locations throughout the complete length of transmission line. The details of all the training combination are given in Table-I as follows:

Table I. Training data for RBFNN

S. No.	Operating fault conditions	Operating Values
1	Fault resistance	0.1, 10, 50, 100 and 150Ω
2	Fault inception angle	0, 45, 60, 90 and 180°
3	Load angle	10, 20, 30, 40 and 50°
4	Fault type	AG, BG, CG, AB, BC, CA, ABG, BCG, CAG, and ABC
5	Voltage Level	230 kV
6	Fault Location	60, 90, 120, 150, 170, 200, 240 and 300 km

Thus, total training data points generated at each location are $5 \times 5 \times 5 \times 10 \times 1 = 1250$ and total numbers of locations taken for data generation are 8 so total numbers of training data patterns are $1250 \times 8 = 10000$. The details of testing patterns for evaluating the classifier performance are given in Table-II.

Table II. Testing data for RBFNN

S. No.	Operating fault conditions	Operating values
1	Fault resistance	0, 60, 100 and 160 Ω
2	Fault inception angle	20, 50, 80, 120 and 150°
3	Load angle	5, 15, 35 and 45°
4	Fault type	AG, AB, BC, ABG, ABC and ABCG
5	Voltage Level	230 kV
6	Fault Location	50, 100, 225 and 275 km

5.1 Effect of noise

In the proposed work line current measured at the receiving end which is associated with the 230 kV voltage. The most severe noise presents in the transmission line is corona noise which significantly affect the current or voltage signal. Corona effect is more severe at higher voltage level. Also the corona noise depends on weather conditions in foul weather it deteriorate. Proposed algorithm is checked for worse possible condition, if corona occurs in the 230kV line in foul weather condition. In this condition corona generates the noise voltage up to 300 mV. For this condition Signal to Noise Ratio (SNR) is worse and the value can be

calculated as: $SNR_{dB} = 20 \log \left[\frac{A_{signal}}{A_{noise}} \right]$ where A is amplitude and the SNR value found to be 117. This SNR has

been added in all the fault patterns assuming that the worst condition is possible in all the cases and trained and tested with RBFNN which nullifies the possibility of any mal-operation if any.

5.2 Performance Comparison and Accuracy

System frequency is 50 Hz and sampling frequency is chosen as 40 kHz such that per cycle samples are 800. RBFNN is tested for $1/16^{\text{th}}$, $1/8^{\text{th}}$ and $1/4^{\text{th}}$ cycle data with different number of samples per cycle. Chosen sampling rate best suited for the purpose and does not impose any memory burden or enormous error to the neural network. RBFNN is tested with all the detailed coefficients (D1 to D4) and number of neurons in hidden layer kept as variable to adjust root mean square error within 0.01. Performance of designed neural network with different window size as 50, 100 and 200 is shown in Table-III.

Table III. RBFNN performance with detailed coefficients

Window Size	Number of hidden layer neurons			
	With D1	With D2	With D3	With D4
50	1538	1028	1087	874
100	408	34	49	76
200	59	54	42	53

It is concluded from Table-III that the structure of neural network is optimum with detailed coefficient D2, with window size 100 sample i.e., the proposed algorithm is very fast and detect fault section within $1/8^{\text{th}}$ cycle time. Performance of neural network with D2 is compared with D1 and error is calculated with some input vector instances for window size 100 and 200 as shown in Fig. 7(a) and 7(b) respectively. Error trajectory amplitude with D2 is found to be less than D1 and it is concluded that with 100 samples window, error curve is smoother than 200 samples as shown in Fig. 7.

Final RBFN network is structured as 100 input neurons, 34 hidden layer neurons and one output. For section-I fault numerical '1' and for section-II faults numerical '0' is assigned. Sigmoidal function with a threshold of 0.5 at output layer adjusts the output value either at '1' or at '0'. Optimize neural network is tested with selected patterns and it is found that the neural network is nearly 100 % accurate. Possibility of misclassification of fault section in mid-point compensated transmission line gradually decreases at different stages. Application of HPF at mid-point creates a major difference in section-I and section-II fault patterns. In next stage WT-MRA confined the various frequency features for analysis on which the decision can be taken. In last stage, RBFNN learned all the conditions adaptively classify the fault section with the possibility of minimum error.

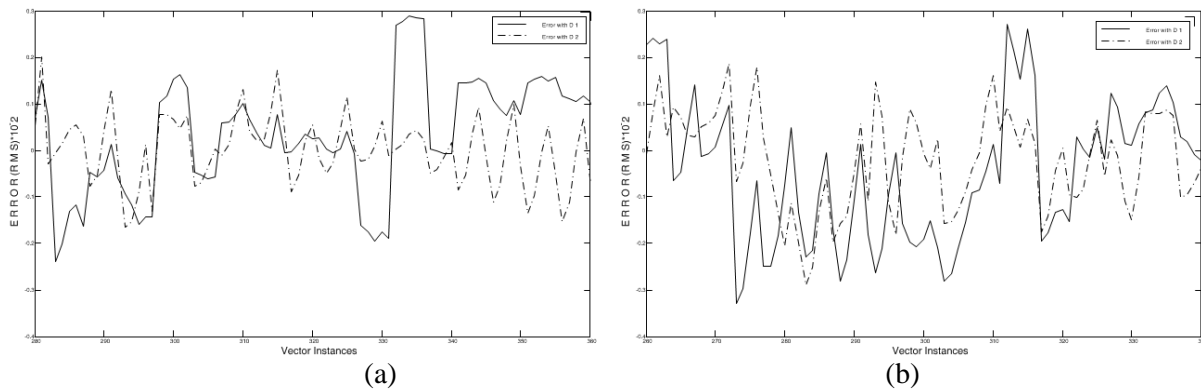


Fig.7. Error curves (a) Window size 100 (b) Window size 200

6. CONCLUSION

The proposed algorithm independently works to the parameters and the mode of operation of compensator. A HPF is installed at the PCC, which filter out all the high frequency components (above 1 kHz), generated during fault in transmission line. DWT-MRA is found to be a powerful tool which breaks fault current into different frequency bands. Mother wavelet 'db4' is chosen for the proposed section identification algorithm. RBFNN analyzes the different frequency bands to take decision whether the fault occurred in section-I or II. The technique has the advantage of cascade filtering at different stages and benefit of adaptive learning which reduce the error. The combined WT-RBFNN techniques successfully classify the fault section with 100 % accuracy.

References:

- [1] R. Mathur and R. Varma, *Thyristor-based FACTS controllers for electrical transmission systems*. Wiley-IEEE Press, 2002.
- [2] N. G. Hingorani and L. Gyugyi, *Understanding FACTS concepts and technology of flexible ac transmission systems*.

- Institute of Electrical and Electronics Engineers, IEEE Press, 2000.
- [3] M. Khederzadeh and T. S. Sidhu, "Impact of TCSC on the protection of transmission lines," *IEEE Transactions on Power Delivery*, vol. 21, no. 1, pp. 80–87, 2006.
 - [4] F. Albasri, T. Sidhu, and R. Varma, "Performance comparison of distance protection schemes for shunt-FACTS compensated transmission lines," *IEEE Transactions on Power Delivery*, vol. 22, no. 4, pp. 2116–2125, 2007.
 - [5] D. Novosel, B. Bachmann, D. Hart, Y. Hu, and M. M. Saha, "Algorithms for Locating Faults on Series Compensated Lines Using Neural Network," *IEEE Transactions on Power Delivery*, vol. 11, no. 4, pp. 1728–1736, 1996.
 - [6] A. I. Megahed, A. M. Moussa, and A. E. Bayoumy, "Usage of Wavelet Transform in the Protection of Series Compensated Transmission Line," *IEEE Transactions on Power Delivery*, vol. 21, no. 3, pp. 1213–1221, 2006.
 - [7] P. K. Dash and S. R. Samantaray, "Phase selection and fault section identification in thyristor controlled series compensated line using discrete wavelet transform," *International Journal of Electrical Power & Energy Systems*, vol. 26, no. 9, pp. 725–732, Nov. 2004.
 - [8] B. Vyas, B. Das, and R. P. Maheshwari, "An improved scheme for identifying fault zone in a series compensated transmission line using undecimated wavelet transform and Chebyshev Neural Network," *International Journal of Electrical Power & Energy Systems*, vol. 63, pp. 760–768, Dec. 2014.
 - [9] Z. Moravej, M. Pazoki, and A. Akbar, "A new approach for fault classification and section detection in compensated transmission line with TCSC," *European Transactions on Electrical Power*, vol. 21, pp. 997–1014, 2011.
 - [10] P. K. Dash, S. R. Samantaray, and G. Panda, "Fault Classification and Section Identification of an Advanced Series Compensated Transmission Line Using Support Vector Machine," *IEEE Transactions on Power Delivery*, vol. 22, no. 1, pp. 67–73, 2007.
 - [11] U. B. Parikh, B. Das, and R. P. Maheshwari, "Combined wavelet-SVM technique for fault zone detection in a series compensated transmission line," *IEEE Transactions on Power Delivery*, vol. 23, no. 4, pp. 1789–1794, 2008.
 - [12] F. Albasri, T. Sidhu, and R. Varma, "Mitigation of adverse effects of midpoint shunt-FACTS compensated transmission lines on distance protection schemes," in *Power Engineering Society*, 2007, pp. 1–8.
 - [13] M. Ghazizadeh-Ahsaei and J. Sadeh, "Accurate fault location algorithm for transmission lines in the presence of shunt-connected flexible AC transmission system devices," *IET Generation Transmission & Distribution*, vol. 6, no. 3, pp. 247–255, 2012.
 - [14] A. Manori, M. Tripathy, and H. O. Gupta, "SVM based zonal setting of Mho relay for shunt compensated transmission line," *International Journal of Electrical Power and Energy Systems*, vol. 78, no. 2016, pp. 422–428, 2016.
 - [15] A. Manori, M. Tripathy, and H. O. Gupta, "An advance compensated Mho relay for protection of TCSC transmission line," *2014 6th IEEE Power India International Conference (PIICON)*, pp. 1–6, 2014.
 - [16] P. Jafarian and M. Sanaye-pasand, "High-Frequency Transients-Based Protection of Multiterminal Transmission Lines Using the SVM Technique," *IEEE Transactions on Power Delivery*, vol. 28, no. 1, pp. 188–196, 2013.
 - [17] C.-L. Liu, "A Tutorial of the Wavelet Transform," pp. 1–72, 2010.
 - [18] I. Daubechies, "Where do wavelets Come From? -A Personal Point of View," *Proceedings of the IEEE*, vol. 84, no. 4, pp. 510–513, 1996.
 - [19] R. N. Mahanty and P. B. D. Gupta, "Application of RBF neural network to fault classification and location in transmission lines," *IEE Proceedings-Generation, Transmission and Distribution*, vol. 151, no. 2, pp. 201–212, 2004.